

# Next-to-Next-to-Leading-Order QCD Prediction for the Pion Form Factor

Yao Ji<sup>a,b,\*</sup>, Bo-Xuan Shi<sup>c,†</sup>, Jian Wang<sup>d,e,‡</sup>, Ye-Fan Wang<sup>f,§</sup>, Yu-Ming Wang<sup>c,¶</sup> and Hui-Xin Yu<sup>c,\*\*</sup>

<sup>a</sup> School of Science and Engineering,  
The Chinese University of Hong Kong,  
Shenzhen, Guangdong, 518172, China

<sup>b</sup> Physik Department T31, James-Franck-Straße1,  
Technische Universität München,  
D-85748 Garching, Germany

<sup>c</sup> School of Physics, Nankai University,  
Weijin Road 94, Tianjin 300071, P.R. China

<sup>d</sup> School of Physics, Shandong University,  
Jinan, Shandong 250100, China

<sup>e</sup> Center for High Energy Physics,  
Peking University, Beijing 100871, China

<sup>f</sup> Department of Physics and Institute of Theoretical Physics,  
Nanjing Normal University,  
Nanjing, Jiangsu 210023, China

(Dated: November 7, 2024)

We accomplish for the first time the two-loop computation of the leading-twist contribution to the pion electromagnetic form factor by employing the effective field theory formalism rigorously. The next-to-next-to-leading-order short-distance matching coefficient is determined by evaluating the appropriate 5-point QCD amplitude with the modern multi-loop technique and subsequently by implementing the ultraviolet renormalization and infrared subtractions with the inclusion of evanescent operators. The renormalization/factorization scale independence of the obtained form factor is then validated explicitly at  $\mathcal{O}(\alpha_s^3)$ . The yielding two-loop QCD correction to this fundamental quantity turns out to be numerically significant at experimentally accessible momentum transfers. We further demonstrate that the newly computed two-loop radiative correction is highly beneficial for an improved determination of the leading-twist pion distribution amplitude.

## INTRODUCTION

It is generally accepted that the pion electromagnetic form factor (EMFF) is of paramount importance for probing the infrared structure of QCD scattering amplitudes of hard exclusive reactions at leading power and beyond and for unraveling the precise mechanisms that dictate the intricate nature of composite hadron systems. Advancing our understanding towards this gold-plated form factor is especially suitable for delivering deep and far-reaching insights into the delicate interplay between the emergent and Higgs mass generation mechanisms for such lightest pseudoscalar mesons as the Nambu-Goldstone modes of QCD. Historically, the systematic analysis of the pion form factor played an indispensable role in establishing the perturbative factorization formalism for the entire domain of exclusive hadronic processes with large momentum transfers [1–7]. As a consequence, the dimensional-counting rules for the power-law behaviour of numerous hard exclusive reactions on the basis of the parton model [8, 9] can be placed on a solid footing within this field-theoretical framework (see [10] for an overview). Additionally, the developed perturbative factorization technique has been extended to the first-principles calculations of the deeply virtual Compton scattering [11–14], the hard diffraction of light

mesons at high energies [15–17], and the exclusive heavy-to-light  $B$ -meson decays at large hadronic recoil [18–21]. Moreover, the time-like scalar-current pion form factors are intimately connected with the chirally-enhanced weak annihilation contributions to the flagship charmless two-body hadronic  $B \rightarrow \pi\pi$  decays [22–24], which provide an essential testing ground for CP violation in the Standard Model (SM) with controllable theoretical uncertainties.

Experimentally, the pion EMFF at low momentum transfers ( $Q^2 \in [0.015, 0.253] \text{ GeV}^2$ ) has been measured from the elastic scattering of high-energy pions off the atomic electrons in a liquid-hydrogen target at Fermilab [25, 26] and CERN [27, 28]. The challenging measurement of the pion form factor at intermediate momentum transfers, up to  $Q^2 = 10 \text{ GeV}^2$ , has been further carried out at Cornell [29–31], DESY [32, 33] and JLab [34–38], by exploiting the so-called Sullivan mechanism and by extrapolating the determined longitudinal cross section at negative values of the Mandelstam variable  $t$  to the pion pole at  $t = m_\pi^2$  [39]. Extracting the charged pion form factor over a wide range of the moderate momentum transfers ( $Q^2 \in [2.0, 6.0] \text{ GeV}^2$ ) can be also anticipated from the E12-06-101 experiment with the upgraded JLab accelerator [40]. Accessing the space-like pion form factor at yet higher momentum transfers ( $10 \text{ GeV}^2 \leq Q^2 \leq 40 \text{ GeV}^2$ ) with high precision will be

one of the key targets for the forthcoming EIC experiment at BNL [41].

According to the hard-collinear factorization theorem [1–6], the leading-power contribution to the pion EMFF in the large-momentum expansion can be expressed in terms of the short-distance matching coefficient and the twist-two light-cone distribution amplitude (LCDA) for the (anti)-collinear pion state. The next-to-leading order (NLO) QCD correction to the perturbatively calculable hard function had been explicitly determined with the diagrammatic factorization approach more than forty years ago [42–46] (see [47] for further verification). Including the complete NLO radiative correction in the factorization analysis of the pion EMFF turns out to be extraordinarily advantageous to pin down the intrinsic theory uncertainty from varying the renormalization and factorization scales in comparison with the counterpart tree-level prediction [47]. Accomplishing the next-to-next-to-leading-order (NNLO) computation of the short-distance coefficient function rigorously is therefore in high demand, on the one hand, for enriching and developing the perturbative factorization formalism at an unprecedented level, and on the other hand, for improving further the resulting theory prediction of the charged pion form factor in order to match the ever-growing precision of the dedicated experimental measurements at JLab and EIC. It is our primary objective to fill such an important and long-standing gap in this Letter, by evaluating an appropriate 5-point partonic matrix element at  $\mathcal{O}(\alpha_s^3)$  with the contemporary advanced multi-loop computational strategies and by carrying out the ultraviolet (UV) renormalization and infrared (IR) subtractions in a meticulous and factorization-compatible manner [48]. Phenomenological implications of the thus determined two-loop QCD correction to the space-like pion form factor at large momentum transfers will be then explored comprehensively, by adopting four sample models for the leading-twist pion distribution amplitude at a low reference scale.

## GENERAL ANALYSIS

We first lay out the theoretical framework for constructing the hard-collinear factorization formula of the pion EMFF at leading power in an expansion in powers of  $\Lambda_{\text{QCD}}^2/Q^2$ , where  $\Lambda_{\text{QCD}}$  stands for the strong interaction scale. Applying the general decomposition for the hadronic matrix element of the quark electromagnetic current enables us to write down

$$\begin{aligned} & \langle \pi^+(p') | j_\mu^{\text{em}}(0) | \pi^+(p) \rangle \\ &= F_\pi(Q^2) (p + p')_\mu + \tilde{F}_\pi(Q^2) (p - p')_\mu, \end{aligned} \quad (1)$$

where  $p$  and  $p'$  correspond to the four-momenta carried by the initial and final pion states, respectively. Employing the vector-current conservation condition imme-

dately leads to  $\tilde{F}_\pi(Q^2) = 0$ , thus leaving us with a single form factor  $F_\pi(Q^2)$ . Implementing further the charge conjugation transformation for the matrix element on the left-hand side of (1) indicates an isospin relation between the two charged pion form factors  $F_{\pi^-}(Q^2) = -F_\pi(Q^2)$  for an arbitrary value of  $Q^2$ . In addition, the electric charge conservation determines the normalization condition for the pion form factor in the forward-scattering limit  $F_\pi(0) = 1$  (see, for instance, [49] for an elementary discussion). Here the customary notation  $Q^2 = -(p - p')^2$  has been employed and the quark electromagnetic current is given by

$$j_\mu^{\text{em}}(x) = \sum_q e_q \bar{q}(x) \gamma_\mu q(x), \quad (2)$$

with  $e_u = 2/3$  and  $e_d = -1/3$  for the up and down quarks. Introducing two light-like reference vectors  $n_\mu$  and  $\bar{n}_\mu$  with the constraints  $n^2 = \bar{n}^2 = 0$  and  $n \cdot \bar{n} = 2$  then allows for the decomposition  $p_\mu = (n \cdot p/2) \bar{n}_\mu$  and  $p'_\mu = (\bar{n} \cdot p'/2) n_\mu$  at the leading-power accuracy.

Taking advantage of the modern effective theory field technique [50, 51], the hard-collinear factorization formula for the pion form factor at large momentum transfers can be cast in the desired form (see [52–56] for an alternative formalism)

$$\begin{aligned} F_\pi(Q^2) &= (e_u - e_d) \frac{4\pi\alpha_s(\nu)}{Q^2} f_\pi^2 \int dx \int dy T_1(x, y, Q^2, \nu, \mu) \\ &\quad \times \phi_\pi(x, \mu) \phi_\pi(y, \mu), \end{aligned} \quad (3)$$

which is valid to all orders in perturbation theory and at leading power in the  $\Lambda_{\text{QCD}}^2/Q^2$  expansion. We take the charged pion decay constant from the three-flavour FLAG average  $f_\pi = (130.2 \pm 1.2)$  MeV [57] with an increased uncertainty from adding an approximate 0.7% charm sea-quark contribution. Apparently, the hard-scattering kernel  $T_1$  depends on both the renormalization scale  $\nu$  and the factorization scale  $\mu$ , the latter of which corresponds to the resolution with which the microscopic structure of the  $\pi$ -meson is being probed. This short-distance coefficient function can be expanded perturbatively in terms of the strong coupling constant (similarly for any other QCD quantity)

$$T_1 = \sum_{\ell=0}^{\infty} \left( \frac{\alpha_s}{4\pi} \right)^\ell T_1^{(\ell)}. \quad (4)$$

The leading-twist pion distribution amplitude  $\phi_\pi$  in the factorized expression (3) can be defined by the renormalized QCD matrix element on the light-cone [58, 59]

$$\begin{aligned} & \langle \pi^+(p') | \bar{u}(\tau \bar{n}) [\tau \bar{n}, 0] \gamma_\mu \gamma_5 d(0) | 0 \rangle \\ &= -i f_\pi p'_\mu \int_0^1 dx e^{ix \tau \bar{n} \cdot p'} \phi_\pi(x, \mu), \end{aligned} \quad (5)$$

where  $[\tau \bar{n}, 0]$  is the finite-length collinear Wilson line ensuring gauge invariance. The one-loop renormalization-group (RG) equation for the light-ray operator on the

left-hand side of (5) implies the conformal partial wave expansion of  $\phi_\pi(x, \mu)$  in terms of the Gegenbauer polynomials with multiplicatively renormalizable coefficients (see [60] for an excellent overview)

$$\phi_\pi(x, \mu) = 6x(1-x) \sum_{m=0}^{\infty} a_m(\mu) C_m^{3/2}(2x-1). \quad (6)$$

The normalization condition  $\int_0^1 dx \phi_\pi(x, \mu) = 1$  has been adopted throughout this work and the odd moments  $a_{1,3,\dots}(\mu)$  vanish due to the G-parity symmetry.

The short-distance matching coefficient  $T_1$  can be routinely determined by investigating the 5-point QCD matrix element below

$$\Pi_\mu = \langle u(p'_1) \bar{d}(p'_2) | j_\mu^{\text{em}}(0) | u(p_1) \bar{d}(p_2) \rangle, \quad (7)$$

where the external momenta can be restricted to their leading components  $p_1 = xp$ ,  $p_2 = \bar{x}p$ ,  $p'_1 = yp'$  and  $p'_2 = \bar{y}p'$  with the “bar notation”  $\bar{x} \equiv 1 - x$ ,  $\bar{y} \equiv 1 - y$ . We will perform the computation of the bare amplitude in dimensional regularization with  $D = 4 - 2\epsilon$ , where UV and IR divergences manifest themselves as poles up to the second order in  $\epsilon$ . The former divergences are evidently cancelled by the UV renormalization for the strong coupling constant  $\alpha_s$  in the  $\overline{\text{MS}}$  scheme, while the latter disappear after executing the nowadays standard IR subtraction procedure.

### NEXT-TO-NEXT-TO-LEADING-ORDER QCD COMPUTATION

We will dedicate this section to a brief technical description of the two-loop QCD calculation for the considered partonic quantity  $\Pi_\mu$ . We start with generating the NNLO Feynman diagrams with **FeynArts** [61] and, independently, by means of an in-house routine. Taking into account the observation that a subset of the two-loop diagrams yield the vanishing contribution, due to the Furry theorem and/or the zero colour (electric) charge factors, we eventually encounter 1066 non-vanishing diagrams of our interest. The two sample Feynman diagrams are depicted in Figure 1 explicitly.

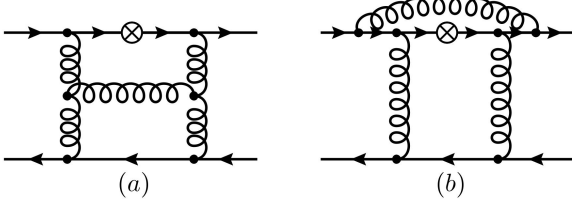


FIG. 1. Sample two-loop Feynman diagrams. The circled cross  $\otimes$  marks an electromagnetic current insertion.

All tensor integrals can be expressed in terms of scalar integrals and algebraic tensorial structures using the Passarino-Veltman decomposition [62]. We then perform the Dirac and tensor reductions with in-house **Mathematica** routines, by applying further the QCD equations of motion and on-shell conditions. The large amount of two-loop scalar integrals are further reduced to an irreducible set of master integrals with the packages **Apart** [63] and **FIRE** [64]. In total, we obtain 57 two-loop master integrals that appear in our computation, 11/16/30 of which appear to depend on 1/2/3 physical scale(s). Unsurprisingly, we encounter the entire list of the 12 one- and two-scale master integrals entering the NNLO computation of the photon-pion form factor [65, 66]. The evaluation of the remaining master integrals can be accomplished in an analytic fashion by employing the method of differential equations [67, 68]. In order to identify a suitable linear transformation such that the master integrals in the new basis satisfy a set of differential equations in an  $\epsilon$ -factorized form (i.e., canonical form) [69], we take advantage of Lee’s algorithm [70] as implemented in the program **Libra** [71]. The boundary conditions to the differential equations are determined by capitalizing on the package **AMFlow** [72] based upon [73, 74]. The yielding numerical results of the master integrals at three distinct kinematic points  $(x, y) \in \{(1/2, 1/5), (1/3, 1/6), (1/4, 1/8)\}$ , with approximately 100 digits, allow us to construct the desired boundary constants of the differential equations in terms of transcendental numbers using the **PSLQ** algorithm [75, 76]. It is thus straightforward to express the master integrals through Goncharov polylogarithms (GPLs) [77, 78] up to the required order in  $\epsilon$ . We will present the analytic expressions for all master integrals in the forthcoming write-up.

### ULTRAVIOLET RENORMALIZATION AND INFRARED SUBTRACTIONS

We proceed to deduce the master formula for the hard-scattering kernel  $T_1$  by performing the UV renormalization and IR subtractions in the presence of evanescent operators, whose significance in the perturbative treatment of quantum field theory has been explored at length ever since the pioneering era of dimensional regularization [79–82]. To achieve this goal, we exploit the matching equation for the interested QCD amplitude  $\Pi_\mu$  onto the effective matrix elements

$$\begin{aligned} \Pi_\mu &= (p + p')_\mu \left[ (e_u - e_d) \frac{4\pi\alpha_s}{Q^4} \sum_k T_k \otimes \langle \mathcal{O}_k \rangle \right], \\ \mathcal{O}_k &\in \{\mathcal{O}_1, \mathcal{O}_2, \mathcal{O}_3\}, \end{aligned} \quad (8)$$

with the following choice of the collinear operator basis

$$\mathcal{O}_1 = [\bar{\chi}_u \not{p} \gamma_5 \chi_d] [\bar{\xi}_d \not{p} \gamma_5 \xi_u],$$

$$\begin{aligned}\mathcal{O}_2 &= [\bar{\chi}_u \gamma_{\perp\alpha} \xi_u] [\bar{\xi}_d \gamma_{\perp}^{\alpha} \chi_d] - \frac{1}{4} \mathcal{O}_1, \\ \mathcal{O}_3 &= [\bar{\chi}_u \gamma_{\perp\alpha} \gamma_{\perp\mu_1} \gamma_{\perp\mu_2} \xi_u] [\bar{\xi}_d \gamma_{\perp}^{\alpha} \gamma_{\perp}^{\mu_2} \gamma_{\perp}^{\mu_1} \chi_d].\end{aligned}\quad (9)$$

One can readily verify that  $\mathcal{O}_1$  is the only physical operator in our problem and the other two operators are evanescent, i.e., vanish algebraically in four dimensions. To reduce our notation to the essentials, we strip off the collinear Wilson lines and the position arguments of quark fields from  $\mathcal{O}_k$ , and represent them merely by their flavour and Dirac structure. Following the conventions of [83], we label the collinear and anti-collinear effective fields moving into the directions of  $\bar{n}$  and  $n$  by  $\xi$  and  $\chi$ , respectively, which evidently satisfy  $\not{n} \xi = 0$  and  $\not{\bar{n}} \chi = 0$ .

We are now in a position to organize the perturbative expansion of the renormalized QCD correlation function  $\Pi_\mu$  in terms of the partonic tree-level matrix elements of the effective operators  $\mathcal{O}_k$

$$\begin{aligned}\Pi_\mu &= (p + p')_\mu (e_u - e_d) \frac{(4\pi)^2}{Q^4} \sum_k \sum_{\ell=1,2,3} \\ &\left[ \left( \frac{Z_\alpha \alpha_s}{4\pi} \right)^{\ell+1} A_k^{(\ell)} \otimes \langle \mathcal{O}_k \rangle^{(0)} \right],\end{aligned}\quad (10)$$

where the renormalization constant of the strong coupling in the standard  $\overline{\text{MS}}$  scheme takes the form of  $Z_\alpha = 1 - \frac{\alpha_s}{4\pi} \frac{1}{\epsilon} \beta_0 + \left( \frac{\alpha_s}{4\pi} \right)^2 \left( \frac{1}{\epsilon^2} \beta_0^2 - \frac{1}{2\epsilon} \beta_1 \right) + \mathcal{O}(\alpha_s^3)$  (see [84–86] for the five-loop expression). The scalar quantities  $A_k^{(\ell)}$  in (10) represent the bare  $\ell$ -loop on-shell QCD amplitudes. In the same vein, the UV-renormalized matrix elements of the collinear operators  $\mathcal{O}_k$  can be expanded according to

$$\langle \mathcal{O}_k \rangle = \sum_i \sum_{\ell=0}^{\infty} \left( \frac{\alpha_s}{4\pi} \right)^\ell Z_{ki}^{(\ell)} \otimes \langle \mathcal{O}_i \rangle^{(0)}, \quad (11)$$

further taking into account that scaleless integrals vanish in dimensional regularization. Since the collinear

fields for distinct directions already decouple at the hard scale, the renormalization constant  $Z_{11}^{(\ell)}$  can be therefore determined from the celebrated Efremov-Radyushkin-Brodsky-Lepage (ERBL) kernel with the one- and two-loop results obtained in [2, 4] and [87–91]. Substituting Eqs. (4), (10) and (11) into the matching equation (8) leads us to derive the master formulae for the short-distance coefficient function

$$\begin{aligned}T_1^{(0)} &= A_1^{(0)}, \\ T_1^{(1)} &= A_1^{(1)} + Z_\alpha^{(1)} A_1^{(0)} - \sum_{k=1,2} Z_{k1}^{(1)} \otimes T_k^{(0)}, \\ T_1^{(2)} &= A_1^{(2)} + 2 Z_\alpha^{(1)} A_1^{(1)} + Z_\alpha^{(2)} A_1^{(0)} \\ &- \sum_{k=1,2,3} \sum_{\ell=1,2} Z_{k1}^{(\ell)} \otimes T_k^{(2-\ell)},\end{aligned}\quad (12)$$

by comparing the coefficient of the tree-level matrix element of the physical operator  $\langle \mathcal{O}_1 \rangle^{(0)}$ . Following the prescription proposed in [92–96], the renormalization constants for the evanescent operators are adjusted to ensure that the IR-finite matrix elements  $\langle \mathcal{O}_k \rangle$  ( $k = 2, 3$ ) vanish at an arbitrary scale. Adopting the preferred collinear operator basis (9) yields the peculiar evanescent-to-physical operator mixing under the RG evolution, which turns out to be adequately captured by the *finite* renormalization constant  $Z_{21}^{(2)}$  at two-loop order. This justifies the essential role of introducing evanescent operators in constructing the QCD factorization formulae with dimensional regularization beyond the leading logarithmic approximation [65, 83, 97–108].

Inserting the newly obtained two-loop expression of the hard-scattering kernel  $T_1$  into the collinear factorization formula (3) and then performing the two-fold integration over  $x \in (0, 1)$  and  $y \in (0, 1)$  analytically with the **Mathematica** package **PolyLogTools** [109] in the asymptotic approximation (namely,  $\phi_\pi^{\text{Asy}}(x, \mu) = 6x(1-x)$ ) results in

---


$$\begin{aligned}F_\pi^{\text{Asy}}(Q^2) &= (e_u - e_d) \frac{4\pi\alpha_s(\nu)}{Q^2} 9 f_\pi^2 \left( \frac{C_F}{2N_c} \right) \left\{ 1 + \left( \frac{\alpha_s}{4\pi} \right) \left[ \beta_0 \ln \frac{\nu^2}{Q^2} + \frac{14}{3} \beta_0 - \frac{71}{6} C_F + \frac{1}{3N_c} \right] \right. \\ &+ \left( \frac{\alpha_s}{4\pi} \right)^2 \left[ \left( \beta_1 \ln \frac{\nu^2}{Q^2} - \beta_0^2 \ln^2 \frac{\nu^2}{Q^2} \right) + 2\beta_0 \ln \frac{\nu^2}{Q^2} \left( \beta_0 \ln \frac{\nu^2}{Q^2} + \frac{14}{3} \beta_0 - \frac{71}{6} C_F + \frac{1}{3N_c} \right) \right. \\ &+ 4 \left( C_F \beta_0 \left( \frac{5}{2} - \zeta_2 \right) - 2 C_F^2 (\zeta_2 + \zeta_3) \right) \ln \frac{\mu^2}{Q^2} + C_A^2 \left( \frac{34873}{81} + \frac{88}{3} \zeta_2 + \frac{152}{3} \zeta_3 - 160 \zeta_5 \right) \\ &- C_A C_F \left( \frac{8191}{18} + \frac{1163}{9} \zeta_2 + 418 \zeta_3 - 2 \zeta_4 - 760 \zeta_5 \right) + C_F^2 (194 + 61 \zeta_2 + 246 \zeta_3 - 18 \zeta_4 - 560 \zeta_5) \\ &\left. \left. - C_A n_\ell T_F \left( \frac{21742}{81} + \frac{32}{3} \zeta_2 - 48 \zeta_3 + \frac{160}{3} \zeta_5 \right) + C_F n_\ell T_F \left( \frac{769}{9} + \frac{316}{9} \zeta_2 - 8 \zeta_3 \right) + (n_\ell T_F)^2 \frac{3496}{81} \right] \right\},\end{aligned}\quad (13)$$


---

where  $C_F = (N_c^2 - 1)/(2N_c)$  and  $C_A = N_c$  denote the

Casimir operators of the fundamental and adjoint rep-

representations of the  $SU(N_c)$  gauge group with the standard normalization  $T_F = 1/2$ . In addition,  $n_\ell$  stands for the number of active quark flavours, and  $\zeta_n$  represents the Riemann zeta function with  $\zeta_2 = \pi^2/6$ ,  $\zeta_3 \cong 1.202056903$ ,  $\zeta_4 = \pi^4/90$ , and  $\zeta_5 \cong 1.036927755$  [110, 111]. Including the higher conformal spin contributions from the twist-two pion LCDA  $\phi_\pi$  leads to the lengthy results for the non-asymptotic corrections to the charged pion form factor, whose explicit expressions with the  $m = 12$  truncation of the Gegenbauer expansion are collected in the Supplemental Material for completeness. In particular, we have verified that the thus achieved NNLO QCD computation of  $F_\pi(Q^2)$  with the perturbative factorization formula (3) is truly independent of the renormalization/factorization scale at the  $\mathcal{O}(\alpha_s^3)$  accuracy, by applying the two-loop evolution equation of  $\phi_\pi(x, \mu)$  [87–91]. Taking advantage of the momentum-space RG formalism enables us to accomplish an all-order summation of the enhanced logarithms of  $Q^2/\Lambda_{\text{QCD}}^2$  entering the factorized expression of  $F_\pi(Q^2)$  in the next-to-next-to-leading-logarithmic (NNLL) approximation, which necessitates an implementation of the three-loop evolution of the leading-twist pion distribution amplitude [112, 113].

## NUMERICAL ANALYSIS

We are now prepared to explore the phenomenological implication of the newly determined two-loop QCD correction to the pion EMFF, with an emphasis on the detailed comparison with both the available experimental measurements and the state-of-the-art lattice QCD results. To achieve this goal, we proceed by first discussing our choice for the phenomenological models of the twist-two pion LCDA appearing in the hard-collinear factorization formula (3). The first model  $\phi_\pi^{\text{Model I}}(x, \mu_0) = [\Gamma(2 + 2\alpha_\pi)/\Gamma^2(1 + \alpha_\pi)] (x\bar{x})^{\alpha_\pi}$  is motivated from the anti-de Sitter-QCD correspondence [114] with the non-perturbative parameter  $\alpha_\pi(\mu_0) = 0.585^{+0.061}_{-0.055}$  [115] determined by matching to the updated lattice result of the second Gegenbauer moment  $a_2(\mu_0) = 0.116^{+0.019}_{-0.020}$  at the reference scale  $\mu_0 = 2.0 \text{ GeV}$  [116]. Our second model  $\{a_2, a_4, a_6, a_8\}(\mu_0) = \{0.181(32), 0.107(36), 0.073(50), 0.022(55)\}$  [117] is obtained from the comparison of the light-cone sum rule for the pion EMFF [118] with the experimental measurements (see [119, 120] for the earlier construction along this line). By contrast, the numerical intervals for the two lowest conformal coefficients in model III  $\{a_2, a_4\}(\mu_0) = \{0.149^{+0.052}_{-0.043}, -0.096^{+0.063}_{-0.058}\}$  [121–123] are extracted from the method of QCD sum rules with non-local condensates [124]. Furthermore, we employ an alternative model (hereafter labelled as model IV) with the first three non-vanishing Gegenbauer coefficients  $\{a_2, a_4, a_6\}(\mu_0) = \{0.196(32), 0.085(26), 0.056(15)\}$  [125] determined from

the lattice prediction for the dynamic shape of the pion distribution amplitude in the range of  $x \in [0.25, 0.75]$  using large momentum effective theory [126–128] and from a simple power-law parametrization of the corresponding end-point behaviour. Additionally, we will vary the renormalization scale for the strong coupling  $\alpha_s$  in the interval  $\nu^2 \in [Q^2/2, 2Q^2]$  with the central value  $Q^2$ . Following [129], the factorization scale  $\mu$  characterizing the virtualities of quark and gluon propagators in the hard-scattering partonic process will be taken as  $\mu^2 = \langle x \rangle Q^2$  with  $1/4 \leq \langle x \rangle \leq 3/4$  (see [47, 104, 130–136] for an elaborate discussion on the renormalization/factorization scale setting).

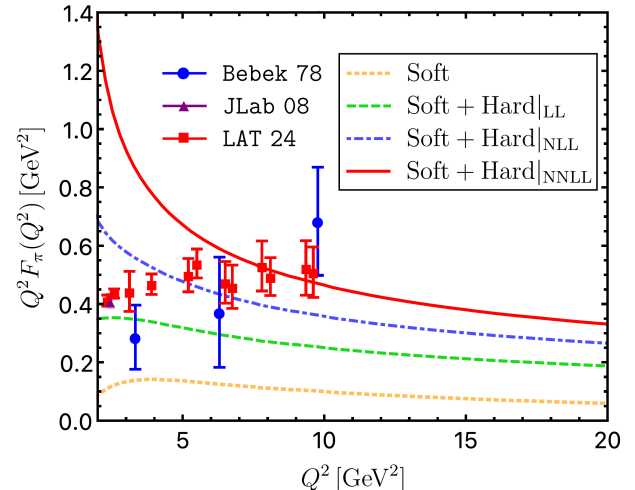


FIG. 2. Theory predictions for the pion EMFF from the soft “end-point” Feynman mechanism [118] (yellow curve) and the (competing) hard-scattering contribution in the kinematic region  $Q^2 \in [2.0, 20.0] \text{ GeV}^2$ . We further collect here the experimental data points for the space-like pion form factor at intermediate momentum transfers (Bebek 78 [31] and JLab 08 [38]) and the most recent lattice QCD predictions with the physical pion mass at  $Q^2 = \{2.34, 2.58, 3.12, 3.90, 5.20, 5.50, 6.50, 6.75, 7.80, 8.10, 9.35, 9.61\} \text{ GeV}^2$  (LAT 24 [137]) for an exploratory comparison.

In order to facilitate an in-depth exploration of the dynamical pattern dictating the pion form factor, we display explicitly in Figure 2 the obtained theory predictions for the leading-power hard-gluon-exchange contributions at leading-logarithmic (LL), NLL, and NNLL accuracy accomplished in this Letter as well as the subleading power corrections arising from I) an atypical “end-point” configuration of twist-two in the one-loop approximation and II) the higher-twist pion distribution amplitudes up to the twist-six accuracy with the dispersion technique [118], by adopting model I of the pion distribution amplitude  $\phi_\pi$  as our default choice. Inspecting the distinctive feature for a variety of higher-order corrections in Figure 2 implies that the newly determined two-loop QCD correction to the hard-scattering contribution based upon the hard-collinear factorization theorem can

substantially enhance the corresponding NLL prediction of the pion form factor at intermediate and large momentum transfers: numerically at the level of  $(30 - 50)\%$ . In analogy to the QCD anatomy of the radiative leptonic  $\bar{B} \rightarrow \gamma \ell \bar{\nu}_\ell$  decay with an energetic photon [138–142], the soft non-factorizable correction to the charged pion form factor can constantly shift the NNLL resummation improved leading-power contribution by approximately an amount of  $\mathcal{O}(25\%)$  in the kinematic domain  $5.0 \text{ GeV}^2 \leq Q^2 \leq 20.0 \text{ GeV}^2$ . We are then led to conclude that an ironclad and *fully analytical* extraction of the two-loop short-distance coefficient function  $T_1^{(2)}$  in the factorized expression (3) is evidently vital for obtaining the robust and accurate theory prediction of the flagship hadron form factor  $F_\pi$  and for advancing further the QCD factorization programme targeting at the high-precision computation of hard exclusive reactions. It remains interesting to observe that the very inclusion of the NNLO QCD correction to the pion EMFF turns out to be especially beneficial for better accommodating the benchmark lattice simulation results at intermediate momentum transfers [137].

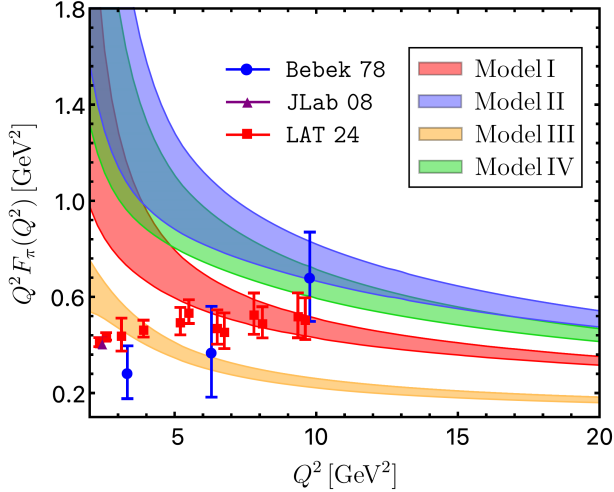


FIG. 3. Theory predictions for the pion EMFF with the four sample models of the leading-twist pion distribution amplitude  $\phi_\pi(x, \mu)$  in the kinematic range  $Q^2 \in [2.0, 20.0] \text{ GeV}^2$  obtained by adding together both the factorizable hard-gluon-exchange contribution at two loops and the various power-suppressed contributions discussed in the text. We also display here the perturbative uncertainties from varying the renormalization and factorization scales in the default intervals as indicated by the colour bands.

We now turn to present in Figure 3 our final theory predictions for the pion form factor  $F_\pi$  with the four different phenomenological models of the twist-two pion LCDA discussed above, confronting with the two experimental measurements **Bebek 78** [31] and **JLab 08** [38] at four distinct kinematic points of  $Q^2 = \{2.45, 3.33, 6.30, 9.77\} \text{ GeV}^2$ . It can then be observed

that the yielding numerical prediction with the anti-de Sitter-QCD inspired model fulfilling an additional constraint from the lattice determination of  $a_2(\mu_0)$  [116] (i.e., our model I) provides us with the most optimized description of the available experimental data points and the model-independent lattice QCD results [137] simultaneously. The extraordinary snapshot of the well-separated uncertainty bands for the first three sample models due to the variations of the renormalization/factorization scales in the preferred intervals is particularly encouraging to acquire new insights on the intricate behaviour of the leading-twist pion distribution amplitude, in combination with the envisaged precision measurements at JLab and EIC. In contrast with the NNLL QCD computation for the photon-pion transition form factor [65, 143], our two-loop prediction of the pion EMFF based upon the hard-collinear factorization prescription approaches the desired scaling behaviour in the formal  $Q^2 \rightarrow \infty$  limit rather slowly. This intriguing pattern can be attributed to the fact that the determined hierarchy between the subleading conformal spin effect and the counterpart asymptotic contribution grows steadily with the increasing loop order  $\ell$  at realistic momentum transfers accessible in the current and forthcoming experimental facilities, thus postponing the onset of the asymptotic regime to an enormously higher value of  $Q^2$  (see [106, 144–146] for further discussions in the context of the nucleon electromagnetic form factors).

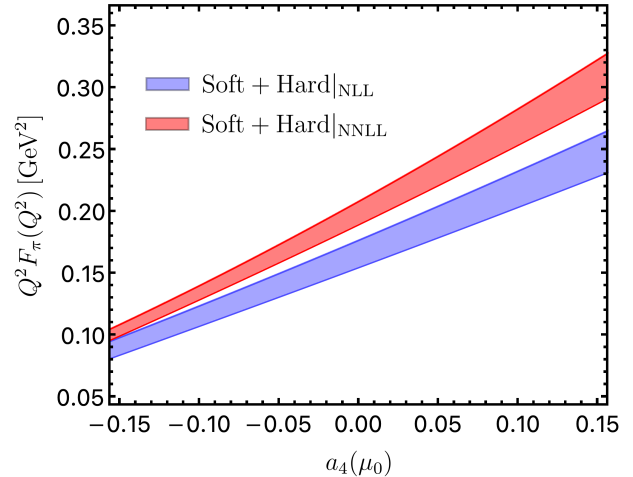


FIG. 4. Theory predictions for the dynamical dependence of the pion EMFF on the fourth conformal coefficient  $a_4(\mu_0)$  of the leading-twist  $\pi$ -meson distribution amplitude at the sample kinematic point  $Q^2 = 30.0 \text{ GeV}^2$ , by taking advantage of the lattice determination of the second Gegenbauer moment from the RQCD Collaboration [116] and by further discarding the higher conformal moments (namely,  $a_{n \geq 6}(\mu_0) = 0$ ) for illustration purposes.

We finally address the genuine benefit of the full two-loop QCD calculation of the charged pion form factor on the model-independent extraction of the shape parame-

ters dictating the twist-two pion distribution amplitude on the light-cone. To this end, we proceed to explore the intrinsic sensitivity of the exclusive  $\pi^+ \gamma^* \rightarrow \pi^+$  form factor on the currently poorly constrained conformal coefficient  $a_4(\mu_0)$  by combining the achieved NNLL prediction of the leading-twist contribution with the previously determined subleading power corrections in the  $\Lambda_{\text{QCD}}^2/Q^2$  expansion. It is evident from Figure 4 that taking into account the newly obtained two-loop QCD correction to the pion EMFF form factor will indeed be advantageous to enhance the sensitivity of extracting the key shape parameter  $a_4(\mu_0)$  in anticipation of the prospective precision EIC measurements [41], complementary to an alternative strategy on the basis of the factorization analysis of the photon-pion form factor [65].

## CONCLUSIONS

In conclusion, we have endeavored to accomplish for the first time the rigorous two-loop QCD computation of the pion form factor in an analytical fashion, by applying the modern effective field theory formalism that enables us to implement the UV renormalization and IR subtractions of evanescent operators systematically. Crucially, we have demonstrated that the thus determined NNLO QCD correction to the short-distance coefficient function can bring about an enormous impact on the pion form factor over a wide range of momentum transfers, by employing the four phenomenologically acceptable models of the leading-twist pion distribution amplitude. In particu-

lar, the very inclusion of the two-loop radiative correction allowed for an improved extraction of the essential shape parameters dictating the intricate profile of the pion distribution amplitude, when confronted with the encouraging measurements from the upcoming EIC experiment. Extending and developing further our factorization prescription to the charged kaon form factor and to the more challenging  $B_c \rightarrow \eta_c \ell \bar{\nu}_\ell$  transition form factors [147–150] will be highly beneficial for deepening our understanding towards the diverse facets of the strong interaction dynamics encoded in the hard-scattering processes.

## ACKNOWLEDGEMENTS

It is our pleasure to thank Yong-Kang Huang for illuminating discussions. The research of Y.J. was supported in part by the Deutsche Forschungsgemeinschaft (DFG, German Research Foundation) through the Sino-German Collaborative Research Center TRR110 “Symmetries and the Emergence of Structure in QCD” (DFG Project-ID 196253076, NSFC Grant No. 12070131001, -TRR 110). J.W. is supported by the National Natural Science Foundation of China with Grant No. 12005117, No. 12321005, and No. 12375076, and the Taishan Scholar Foundation of Shandong province with Grant No. TSQN201909011. The work of Y.F.W. is supported in part by the National Natural Science Foundation of China with Grant No. 12405117. Y.M.W. acknowledges support from the National Natural Science Foundation of China with Grant No. 12075125 and No. 2475097.

## SUPPLEMENTAL MATERIAL

Here we collect the general expression for the derived two-loop pion electromagnetic form factor with the inclusion of the non-asymptotic corrections

$$\begin{aligned}
F_\pi(Q^2) = & (e_u - e_d) \frac{4\pi\alpha_s(\nu)}{Q^2} 9 f_\pi^2 \left( \frac{C_F}{2N_c} \right) \sum_{m=0,2,4,\dots} \sum_{n=0,2,4,\dots} a_m(\mu) a_n(\mu) \\
& \times \left\{ 1 + \left( \frac{\alpha_s}{4\pi} \right) \left[ \beta_0 \ln \frac{\nu^2}{Q^2} + (\gamma_{m,m}^{(0)} + \gamma_{n,n}^{(0)}) \ln \frac{\mu^2}{Q^2} + \mathcal{R}_{mn}^{(1)} \right] \right. \\
& + \left( \frac{\alpha_s}{4\pi} \right)^2 \left[ \left( \beta_1 \ln \frac{\nu^2}{Q^2} - \beta_0^2 \ln^2 \frac{\nu^2}{Q^2} \right) + 2\beta_0 \ln \frac{\nu^2}{Q^2} \left( \beta_0 \ln \frac{\nu^2}{Q^2} + (\gamma_{m,m}^{(0)} + \gamma_{n,n}^{(0)}) \ln \frac{\mu^2}{Q^2} + \mathcal{R}_{m,n}^{(1)} \right) \right. \\
& + \left( \sum_{m'=m}^{\infty} \gamma_{m',m}^{(1)} + \sum_{n'=n}^{\infty} \gamma_{n',n}^{(1)} \right) \ln \frac{\mu^2}{Q^2} - \frac{1}{2} \left( (\gamma_{m,m}^{(0)} + \gamma_{n,n}^{(0)})^2 + \beta_0 (\gamma_{m,m}^{(0)} + \gamma_{n,n}^{(0)}) \right) \ln^2 \frac{\mu^2}{Q^2} \\
& + (\gamma_{m,m}^{(0)} + \gamma_{n,n}^{(0)}) \ln \frac{\mu^2}{Q^2} \left( \beta_0 \ln \frac{\nu^2}{Q^2} + (\gamma_{m,m}^{(0)} + \gamma_{n,n}^{(0)}) \ln \frac{\mu^2}{Q^2} + \mathcal{R}_{m,n}^{(1)} \right) \\
& \left. - \beta_0 \ln \frac{\nu^2}{Q^2} (\gamma_{m,m}^{(0)} + \gamma_{n,n}^{(0)}) \ln \frac{\mu^2}{Q^2} + \mathcal{R}_{m,n}^{(2)} \right] + \mathcal{O}(\alpha_s^3) \Big\}, \tag{14}
\end{aligned}$$

by inserting the Gegenbauer expansion of the pion distribution amplitude (6) into the hard-collinear factorization formula (3) and then by evaluating the double convolution integrals over the quark momentum fractions analytically. We can readily verify that the two coefficient matrices  $\gamma^{(0)}$  and  $\gamma^{(1)}$  coincide with the one- and two-loop anomalous dimensions (apart from an overall minus sign) of the flavour-octet local operators defining the conformal moments of the twist-two distribution amplitude  $\phi_\pi$ . The explicit expressions of these anomalous dimensions are given by [151]

$$\begin{aligned}\gamma_{m,n}^{(0)} &= \gamma_m^{(0)} \delta_{mn} = C_F \left[ 4 S_1(m+1) - \frac{2}{(m+1)(m+2)} - 3 \right] \delta_{mn}, \\ \gamma_{m,n}^{(1)} &= \gamma_m^{(1)} \delta_{mn} + \frac{(n+1)(n+2)}{(m+1)(m+2)} \frac{\gamma_m^{(0)} - \gamma_n^{(0)}}{\mathbf{a}(m,n)} \left[ 2(2m+3) (\beta_0 + \gamma_n^{(0)}) - \frac{2m+3}{2n+3} \mathbf{w}_{m,n}^{(0)} \right] \vartheta_{mn},\end{aligned}\quad (15)$$

where we have introduced the following definitions and conventions [112, 113, 152]

$$\begin{aligned}S_\ell(m) &= \sum_{k=1}^m \frac{1}{k^\ell}, \quad S'_\ell(m) = 2^{\ell-1} \sum_{k=1}^m [1 + (-1)^k] \frac{1}{k^\ell}, \quad \tilde{S}(m) = \sum_{k=1}^m \frac{(-1)^k}{k^2} S_1(k), \\ \mathbf{a}(m,n) &= (m-n)(m+n+3), \quad \vartheta_{mn} = \begin{cases} 1 & \text{if } m-n > 0 \text{ and even} \\ 0 & \text{else.} \end{cases}\end{aligned}\quad (16)$$

It is straightforward to express the diagonal two-loop anomalous dimensions in terms of the preceding harmonic sums

$$\begin{aligned}\gamma_m^{(1)} &= 2 \left( C_F^2 - \frac{1}{2} C_F C_A \right) \left[ \frac{4(2m+3)}{(m+1)^2(m+2)^2} S_1(m+1) - 2 \frac{3m^3 + 10m^2 + 11m + 3}{(m+1)^3(m+2)^3} \right. \\ &\quad + 4 \left( 2S_1(m+1) - \frac{1}{(m+1)(m+2)} \right) (S_2(m+1) - S'_2(m+1)) + 16 \tilde{S}(m+1) \\ &\quad + 6S_2(m+1) - \frac{3}{4} - 2S'_3(m+1) - 4(-1)^{m+1} \frac{2m^2 + 6m + 5}{(m+1)^3(m+2)^3} \Big] \\ &\quad + 2C_F C_A \left[ S_1(m+1) \left( \frac{134}{9} + \frac{2(2m+3)}{(m+1)^2(m+2)^2} \right) - 4S_1(m+1)S_2(m+1) \right. \\ &\quad + S_2(m+1) \left( -\frac{13}{3} + \frac{2}{(m+1)(m+2)} \right) - \frac{43}{24} - \frac{1}{9} \frac{151m^4 + 867m^3 + 1792m^2 + 1590m + 523}{(m+1)^3(m+2)^3} \Big] \\ &\quad \left. + 2C_F n_\ell T_F \left[ -\frac{40}{9} S_1(m+1) + \frac{8}{3} S_2(m+1) + \frac{1}{3} + \frac{4}{9} \frac{11m^2 + 27m + 13}{(m+1)^2(m+2)^2} \right] \right].\end{aligned}\quad (17)$$

The non-trivial matrix  $\mathbf{w}^{(0)}$  arises from the one-loop conformal anomaly [112]

$$\mathbf{w}_{mn}^{(0)} = 4C_F (2n+3) \mathbf{a}(m,n) \left[ \frac{A_{mn} - S_1(m+1)}{(n+1)(n+2)} + \frac{2A_{mn}}{\mathbf{a}(m,n)} \right], \quad (18)$$

where

$$A_{mn} = S_1 \left( \frac{m+n+2}{2} \right) - S_1 \left( \frac{m-n-2}{2} \right) + 2S_1(m-n-1) - S_1(m+1). \quad (19)$$

We now turn to present the desired expressions for the scattering kernels  $\mathcal{R}^{(1)}$  and  $\mathcal{R}^{(2)}$  by truncating the Gegenbauer expansion (6) at  $m=12$  (which is sufficient for practical purposes)

$$\begin{aligned}\mathcal{R}_{0,0}^{(1)} &= \frac{79}{3}, & \mathcal{R}_{2,0}^{(1)} &= \frac{2959}{54} - 4\zeta_3, \\ \mathcal{R}_{2,2}^{(1)} &= \frac{20563}{252} + \frac{24}{7}\zeta_3, & \mathcal{R}_{4,0}^{(1)} &= \frac{47537}{675} - 4\zeta_3, \\ \mathcal{R}_{4,2}^{(1)} &= \frac{732221}{5400} - 24\zeta_3, & \mathcal{R}_{4,4}^{(1)} &= \frac{674701}{7425} + \frac{360}{11}\zeta_3, \\ \mathcal{R}_{6,0}^{(1)} &= \frac{130661509}{1587600} - 4\zeta_3, & \mathcal{R}_{6,2}^{(1)} &= \frac{239823149}{1587600} - 24\zeta_3, \\ \mathcal{R}_{6,4}^{(1)} &= \frac{348346949}{1587600} - 60\zeta_3, & \mathcal{R}_{6,6}^{(1)} &= \frac{244715911}{7938000} + 112\zeta_3,\end{aligned}\quad (20)$$

$$\begin{aligned}
\mathcal{R}_{8,0}^{(1)} &= \frac{109546973}{1190700} - 4\zeta_3, \\
\mathcal{R}_{8,4}^{(1)} &= \frac{4439757281}{19051200} - 60\zeta_3, \\
\mathcal{R}_{8,8}^{(1)} &= -\frac{7475238623}{60328800} + \frac{5040}{19}\zeta_3, \\
\mathcal{R}_{10,2}^{(1)} &= \frac{1002154859077}{5762988000} - 24\zeta_3, \\
\mathcal{R}_{10,6}^{(1)} &= \frac{209131003489}{640332000} - 112\zeta_3, \\
\mathcal{R}_{10,10}^{(1)} &= -\frac{61920191868971}{154640178000} + \frac{11880}{23}\zeta_3, \\
\mathcal{R}_{12,2}^{(1)} &= \frac{267253043878417}{1460917458000} - 24\zeta_3, \\
\mathcal{R}_{12,6}^{(1)} &= \frac{1969363800385939}{5843669832000} - 112\zeta_3, \\
\mathcal{R}_{12,10}^{(1)} &= \frac{22456093016133983}{40905688824000} - 264\zeta_3, \\
\mathcal{R}_{8,2}^{(1)} &= \frac{3114185693}{19051200} - 24\zeta_3, \\
\mathcal{R}_{8,6}^{(1)} &= \frac{29960812963}{95256000} - 112\zeta_3, \\
\mathcal{R}_{10,0}^{(1)} &= \frac{77040022223}{768398400} - 4\zeta_3, \\
\mathcal{R}_{10,4}^{(1)} &= \frac{352200966463}{1440747000} - 60\zeta_3, \\
\mathcal{R}_{10,8}^{(1)} &= \frac{11399947544291}{26893944000} - 180\zeta_3, \\
\mathcal{R}_{12,0}^{(1)} &= \frac{125618726214131}{1168733966400} - 4\zeta_3, \\
\mathcal{R}_{12,4}^{(1)} &= \frac{743080051414439}{2921834916000} - 60\zeta_3, \\
\mathcal{R}_{12,8}^{(1)} &= \frac{2963676052586981}{6817614804000} - 180\zeta_3, \\
\mathcal{R}_{12,12}^{(1)} &= -\frac{65202266056847263}{78889542732000} + \frac{8008}{9}\zeta_3,
\end{aligned} \tag{21}$$

and

$$\begin{aligned}
\mathcal{R}_{0,0}^{(2)} &= \frac{13136}{9} - \frac{1100}{9}\zeta_2 - \frac{1736}{3}\zeta_3 - 24\zeta_4 + \frac{3280}{9}\zeta_5, \\
\mathcal{R}_{2,0}^{(2)} &= \frac{254500067}{58320} - \frac{23684}{81}\zeta_2 - \frac{429964}{405}\zeta_3 - \frac{1072}{27}\zeta_4 + \frac{1240}{9}\zeta_5 - \frac{64}{3}\zeta_2\zeta_3, \\
\mathcal{R}_{2,2}^{(2)} &= -\frac{977775959}{2857680} - \frac{148996}{567}\zeta_2 - \frac{163637624}{6615}\zeta_3 - \frac{464}{63}\zeta_4 + \frac{750200}{21}\zeta_5 + \frac{128}{7}\zeta_2\zeta_3, \\
\mathcal{R}_{4,0}^{(2)} &= \frac{257785535129}{40824000} - \frac{740213}{2025}\zeta_2 - \frac{76336859}{56700}\zeta_3 - \frac{5588}{135}\zeta_4 + \frac{1420}{9}\zeta_5 - \frac{64}{3}\zeta_2\zeta_3, \\
\mathcal{R}_{4,2}^{(2)} &= \frac{1065085696391}{61236000} - \frac{2216813}{2025}\zeta_2 - \frac{25432877}{4725}\zeta_3 - \frac{6776}{45}\zeta_4 + \frac{2440}{3}\zeta_5 - 128\zeta_2\zeta_3, \\
\mathcal{R}_{4,4}^{(2)} &= -\frac{11028087335760793}{148191120000} + \frac{4090648}{7425}\zeta_2 - \frac{8897578969}{38115}\zeta_3 + \frac{5360}{33}\zeta_4 + \frac{3894200}{11}\zeta_5 + \frac{1920}{11}\zeta_2\zeta_3, \\
\mathcal{R}_{6,0}^{(2)} &= \frac{836512595865907}{105019740000} - \frac{500357213}{1190700}\zeta_2 - \frac{307464947}{198450}\zeta_3 - \frac{13394}{315}\zeta_4 + \frac{560}{3}\zeta_5 - \frac{64}{3}\zeta_2\zeta_3, \\
\mathcal{R}_{6,2}^{(2)} &= \frac{301245598893433619}{13862605680000} - \frac{469249769}{396900}\zeta_2 - \frac{14861306149}{2182950}\zeta_3 - \frac{49564}{315}\zeta_4 + \frac{7840}{9}\zeta_5 - 128\zeta_2\zeta_3, \\
\mathcal{R}_{6,4}^{(2)} &= \frac{404162543588361839}{11263367115000} - \frac{7248599}{2940}\zeta_2 - \frac{75906747509}{5675670}\zeta_3 - \frac{24110}{63}\zeta_4 + \frac{17920}{9}\zeta_5 - 320\zeta_2\zeta_3, \\
\mathcal{R}_{6,6}^{(2)} &= -\frac{1225342905440097358661}{3003564564000000} + \frac{10130732267}{2976750}\zeta_2 - \frac{2240710975609}{2027025}\zeta_3 + \frac{30472}{45}\zeta_4 + \frac{15187760}{9}\zeta_5 \\
&\quad + \frac{1792}{3}\zeta_2\zeta_3,
\end{aligned} \tag{22}$$

$$\begin{aligned}
\mathcal{R}_{8,0}^{(2)} &= \frac{37633208029413760787}{3992430435840000} - \frac{110645531}{238140}\zeta_2 - \frac{44934684233}{26195400}\zeta_3 - \frac{24592}{567}\zeta_4 + \frac{2020}{9}\zeta_5 - \frac{64}{3}\zeta_2\zeta_3, \\
\mathcal{R}_{8,2}^{(2)} &= \frac{163112130688903608307}{6487699458240000} - \frac{178296143}{142884}\zeta_2 - \frac{3081644849093}{397296900}\zeta_3 - \frac{30704}{189}\zeta_4 + \frac{2840}{3}\zeta_5 - 128\zeta_2\zeta_3, \\
\mathcal{R}_{8,4}^{(2)} &= \frac{2254739676926391897989}{51901595665920000} - \frac{4575297001}{1786050}\zeta_2 - \frac{781344803377}{45405360}\zeta_3 - \frac{74744}{189}\zeta_4 + \frac{6200}{3}\zeta_5 - 320\zeta_2\zeta_3, \\
\mathcal{R}_{8,6}^{(2)} &= \frac{481102607081572963427}{8109624322800000} - \frac{53979658807}{11907000}\zeta_2 - \frac{1404431436769}{56756700}\zeta_3 - \frac{303344}{405}\zeta_4 + \frac{33160}{9}\zeta_5 - \frac{1792}{3}\zeta_2\zeta_3, \\
\mathcal{R}_{8,8}^{(2)} &= -\frac{180398275019354202293598809}{131155332247779840000} + \frac{323163339253}{33934950}\zeta_2 - \frac{14833184489256277}{4097833740}\zeta_3 + \frac{299176}{171}\zeta_4 + \frac{105065000}{19}\zeta_5 \\
&\quad + \frac{26880}{19}\zeta_2\zeta_3,
\end{aligned}$$

$$\begin{aligned}
\mathcal{R}_{10,0}^{(2)} &= \frac{1856383457381690687076503}{172702559578348800000} - \frac{72378211243}{144074700} \zeta_2 - \frac{697029440729}{374594220} \zeta_3 - \frac{1373924}{31185} \zeta_4 + \frac{2440}{9} \zeta_5 - \frac{64}{3} \zeta_2 \zeta_3, \\
\mathcal{R}_{10,2}^{(2)} &= \frac{606035400964911136878473}{21587819947293600000} - \frac{2810106246419}{2161120500} \zeta_2 - \frac{14893752681371}{1748106360} \zeta_3 - \frac{1731448}{10395} \zeta_4 + 1040 \zeta_5 - 128 \zeta_2 \zeta_3, \\
\mathcal{R}_{10,4}^{(2)} &= \frac{2105883569365437834152149}{43175639894587200000} - \frac{5694381908423}{2161120500} \zeta_2 - \frac{90117596993}{4624620} \zeta_3 - \frac{843548}{2079} \zeta_4 + 2160 \zeta_5 - 320 \zeta_2 \zeta_3, \\
\mathcal{R}_{10,6}^{(2)} &= \frac{2014029806290297262575518833}{27891463371903331200000} - \frac{10031992103341}{2161120500} \zeta_2 - \frac{33180462838087841}{1008282775500} \zeta_3 - \frac{684448}{891} \zeta_4 + \frac{34000}{9} \zeta_5 \\
&\quad - \frac{1792}{3} \zeta_2 \zeta_3, \\
\mathcal{R}_{10,8}^{(2)} &= \frac{1060110794989443086553539773}{12202515225207707400000} - \frac{55755464247419}{7563921750} \zeta_2 - \frac{23461093286572259}{604969665300} \zeta_3 - \frac{290672}{231} \zeta_4 + \frac{17680}{3} \zeta_5 \\
&\quad - 960 \zeta_2 \zeta_3, \\
\mathcal{R}_{10,10}^{(2)} &= -\frac{7623163052247813164197161161}{2113433554775142600000} + \frac{3521098742449999}{173970200250} \zeta_2 - \frac{4038145298287288999}{427846193775} \zeta_3 + \frac{1741904}{483} \zeta_4 \\
&\quad + \frac{331478840}{23} \zeta_5 + \frac{63360}{23} \zeta_2 \zeta_3, \\
\mathcal{R}_{12,0}^{(2)} &= \frac{27238692085662585312666509011}{2276565140361793881600000} - \frac{58662551981653}{109568809350} \zeta_2 - \frac{3328917505379}{1669619952} \zeta_3 - \frac{18093512}{405405} \zeta_4 + \frac{980}{3} \zeta_5 \\
&\quad - \frac{64}{3} \zeta_2 \zeta_3, \\
\mathcal{R}_{12,2}^{(2)} &= \frac{9275362166959330623335552267}{302356307704300749900000} - \frac{1472748757823173}{1095688093500} \zeta_2 - \frac{34886708137087}{3801366855} \zeta_3 - \frac{22973824}{135135} \zeta_4 + \frac{10360}{9} \zeta_5 \\
&\quad - 128 \zeta_2 \zeta_3, \\
\mathcal{R}_{12,4}^{(2)} &= \frac{39131838489042454388302002242581}{735330540336859423756800000} - \frac{2951046406156861}{1095688093500} \zeta_2 - \frac{10743538046061211}{505581791715} \zeta_3 - \frac{11198624}{27027} \zeta_4 \\
&\quad + \frac{20440}{9} \zeta_5 - 320 \zeta_2 \zeta_3, \\
\mathcal{R}_{12,6}^{(2)} &= \frac{7370624376245151247754283251569}{91916317542107427969600000} - \frac{1479636772346807}{313053741000} \zeta_2 - \frac{628083708662162821}{16852726390500} \zeta_3 - \frac{9083824}{11583} \zeta_4 \\
&\quad + \frac{35000}{9} \zeta_5 - \frac{1792}{3} \zeta_2 \zeta_3, \\
\mathcal{R}_{12,8}^{(2)} &= \frac{2135300631885046576864376162630941}{19731369499039061204140800000} - \frac{14371610356485754}{1917454163625} \zeta_2 - \frac{29274971196758882773}{542657789774100} \zeta_3 - \frac{1285412}{1001} \zeta_4 \\
&\quad + \frac{54040}{9} \zeta_5 - 960 \zeta_2 \zeta_3, \\
\mathcal{R}_{12,10}^{(2)} &= \frac{34759246718509381395382960927377323}{295970542485585918062112000000} - \frac{84601386041751247}{7669816654500} \zeta_2 - \frac{73968520281383371781}{1356644474435250} \zeta_3 \\
&\quad - \frac{23555288}{12285} \zeta_4 + \frac{77560}{9} \zeta_5 - 1408 \zeta_2 \zeta_3, \\
\mathcal{R}_{12,12}^{(2)} &= -\frac{20233840212533868013654477744867770453}{25115214605205433618413504000000} + \frac{6748656400305647}{182614682250} \zeta_2 - \frac{2829435642800818984903}{134173629339750} \zeta_3 \\
&\quad + \frac{23637968}{3645} \zeta_4 + \frac{868886200}{27} \zeta_5 + \frac{128128}{27} \zeta_2 \zeta_3. \tag{23}
\end{aligned}$$

It remains important to point out the interesting relations  $\mathcal{R}_{m,n}^{(1)} = \mathcal{R}_{n,m}^{(1)}$  and  $\mathcal{R}_{m,n}^{(2)} = \mathcal{R}_{n,m}^{(2)}$  on account of the charge-conjugation symmetry of the pion form factor.

<sup>\*</sup> corresponding author: yao.ji@tum.de

<sup>†</sup> corresponding author: shibx@mail.nankai.edu.cn

<sup>‡</sup> corresponding author: j.wang@sdu.edu.cn

<sup>§</sup> corresponding author: wangyefan@nnu.edu.cn

<sup>¶</sup> corresponding author: wangyuming@nankai.edu.cn

\*\* corresponding author: yuhuixin@mail.nankai.edu.cn

[1] G. P. Lepage and S. J. Brodsky, Phys. Lett. B **87**, 359 (1979).

[2] G. P. Lepage and S. J. Brodsky, Phys. Rev. D **22**, 2157 (1980).

[3] A. V. Efremov and A. V. Radyushkin, Theor. Math. Phys. **42**, 97 (1980).

- [4] A. V. Efremov and A. V. Radyushkin, Phys. Lett. B **94**, 245 (1980).
- [5] A. Duncan and A. H. Mueller, Phys. Rev. D **21**, 1636 (1980).
- [6] A. Duncan and A. H. Mueller, Phys. Lett. B **90**, 159 (1980).
- [7] S. J. Brodsky and G. P. Lepage, Adv. Ser. Direct. High Energy Phys. **5**, 93 (1989).
- [8] S. J. Brodsky and G. R. Farrar, Phys. Rev. Lett. **31**, 1153 (1973).
- [9] V. A. Matveev, R. M. Muradian, and A. N. Tavkhelidze, Lett. Nuovo Cim. **7**, 719 (1973).
- [10] F. Gross *et al.*, Eur. Phys. J. C **83**, 1125 (2023), arXiv:2212.11107 [hep-ph].
- [11] X.-D. Ji, Phys. Rev. D **55**, 7114 (1997), arXiv:hep-ph/9609381.
- [12] A. V. Radyushkin, Phys. Rev. D **56**, 5524 (1997), arXiv:hep-ph/9704207.
- [13] M. Diehl, T. Feldmann, R. Jakob, and P. Kroll, Phys. Lett. B **460**, 204 (1999), arXiv:hep-ph/9903268.
- [14] M. Diehl, T. Feldmann, R. Jakob, and P. Kroll, Eur. Phys. J. C **8**, 409 (1999), arXiv:hep-ph/9811253.
- [15] J. C. Collins, L. Frankfurt, and M. Strikman, Phys. Rev. D **56**, 2982 (1997), arXiv:hep-ph/9611433.
- [16] S. J. Brodsky, L. Frankfurt, J. F. Gunion, A. H. Mueller, and M. Strikman, Phys. Rev. D **50**, 3134 (1994), arXiv:hep-ph/9402283.
- [17] B. Pire, K. Semenov-Tian-Shansky, and L. Szymanowski, Phys. Rept. **940**, 1 (2021), arXiv:2103.01079 [hep-ph].
- [18] M. Beneke and T. Feldmann, Nucl. Phys. B **592**, 3 (2001), arXiv:hep-ph/0008255.
- [19] M. Beneke and T. Feldmann, Nucl. Phys. B **685**, 249 (2004), arXiv:hep-ph/0311335.
- [20] C. W. Bauer, S. Fleming, D. Pirjol, and I. W. Stewart, Phys. Rev. D **63**, 114020 (2001), arXiv:hep-ph/0011336.
- [21] C. W. Bauer, D. Pirjol, and I. W. Stewart, Phys. Rev. D **67**, 071502 (2003), arXiv:hep-ph/0211069.
- [22] M. Beneke, G. Buchalla, M. Neubert, and C. T. Sachrajda, Nucl. Phys. B **606**, 245 (2001), arXiv:hep-ph/0104110.
- [23] M. Duraisamy and A. L. Kagan, Eur. Phys. J. C **70**, 921 (2010), arXiv:0812.3162 [hep-ph].
- [24] C.-D. Lü, Y.-L. Shen, C. Wang, and Y.-M. Wang, Nucl. Phys. B **990**, 116175 (2023), arXiv:2202.08073 [hep-ph].
- [25] E. B. Dally *et al.*, Phys. Rev. D **24**, 1718 (1981).
- [26] E. B. Dally *et al.*, Phys. Rev. Lett. **48**, 375 (1982).
- [27] S. R. Amendolia *et al.*, Phys. Lett. B **146**, 116 (1984).
- [28] S. R. Amendolia *et al.* (NA7), Nucl. Phys. B **277**, 168 (1986).
- [29] C. J. Bebek, C. N. Brown, M. Herzlinger, S. D. Holmes, C. A. Lichtenstein, F. M. Pipkin, S. Raither, and L. K. Sisterson, Phys. Rev. D **13**, 25 (1976).
- [30] C. J. Bebek *et al.*, Phys. Rev. Lett. **37**, 1326 (1976).
- [31] C. J. Bebek *et al.*, Phys. Rev. D **17**, 1693 (1978).
- [32] P. Brauel, T. Canzler, D. Cordes, R. Felst, G. Grindhammer, M. Helm, W. D. Kollmann, H. Krebs, and M. Schadlich, Z. Phys. C **3**, 101 (1979).
- [33] H. Ackermann, T. Azemoon, W. Gabriel, H. D. Mertens, H. D. Reich, G. Specht, F. Janata, and D. Schmidt, Nucl. Phys. B **137**, 294 (1978).
- [34] J. Volmer *et al.* (Jefferson Lab F(pi)), Phys. Rev. Lett. **86**, 1713 (2001), arXiv:nucl-ex/0010009.
- [35] V. Tadevosyan *et al.* (Jefferson Lab F(pi)), Phys. Rev. C **75**, 055205 (2007), arXiv:nucl-ex/0607007.
- [36] T. Horn *et al.* (Jefferson Lab F(pi)-2), Phys. Rev. Lett. **97**, 192001 (2006), arXiv:nucl-ex/0607005.
- [37] H. P. Blok *et al.* (Jefferson Lab), Phys. Rev. C **78**, 045202 (2008), arXiv:0809.3161 [nucl-ex].
- [38] G. M. Huber *et al.* (Jefferson Lab), Phys. Rev. C **78**, 045203 (2008), arXiv:0809.3052 [nucl-ex].
- [39] J. D. Sullivan, Phys. Rev. D **5**, 1732 (1972).
- [40] J. Arrington *et al.*, Prog. Part. Nucl. Phys. **127**, 103985 (2022), arXiv:2112.00060 [nucl-ex].
- [41] R. Abdul Khalek *et al.*, Nucl. Phys. A **1026**, 122447 (2022), arXiv:2103.05419 [physics.ins-det].
- [42] R. D. Field, R. Gupta, S. Otto, and L. Chang, Nucl. Phys. B **186**, 429 (1981).
- [43] F. M. Dittes and A. V. Radyushkin, Sov. J. Nucl. Phys. **34**, 293 (1981).
- [44] M. H. Sarmadi, *The asymptotic pion form factor to the leading order and beyond*, Ph.d. thesis (1982).
- [45] R. S. Khalmuradov and A. V. Radyushkin, Sov. J. Nucl. Phys. **42**, 289 (1985).
- [46] E. Braaten and S.-M. Tse, Phys. Rev. D **35**, 2255 (1987).
- [47] B. Melic, B. Nizic, and K. Passek, Phys. Rev. D **60**, 074004 (1999), arXiv:hep-ph/9802204.
- [48] We note that an earlier attempt to carry out the two-loop QCD computation of the pion electromagnetic form factor at leading power in the  $\Lambda_{\text{QCD}}^2/Q^2$  expansion was made in the work [153], by applying the light-cone projections on the leading-twist (anti)-collinear operators before performing the UV renormalization for the bare 5-point QCD matrix element. As extensively discussed in the factorization analysis of exclusive heavy-quark hadron decays [83, 97–100], such projections do not necessarily commute with the  $\overline{\text{MS}}$  renormalization for the considered bare QCD amplitude. Consequently, the practical prescription implemented in [153] cannot be rigorously justified in the perturbative factorization framework (see [65, 101–108, 154, 155] for additional discussions). In particular, it is insufficient to provide the results of the short-distance matching coefficients in the operator-product-expansion programme without specifying the very definition of evanescent operators, as already emphasized in the comprehensive textbooks [82, 156]. Moreover, these authors failed to demonstrate the renormalization/factorization scale independence of the obtained pion form factor at two-loop order, since they did not take into account the UV renormalization of the strong coupling constant  $\alpha_s$  in an appropriate manner in the published version of [153]. In the revised preprint version <https://arxiv.org/pdf/2312.17228.pdf>, the authors explicitly admitted that they made this mistake in extracting the renormalized hard matching coefficient at  $\mathcal{O}(\alpha_s^3)$ , thus affecting the obtained numerical prediction for the two-loop QCD correction to the pion form factor substantially.
- [49] A. Khodjamirian, *Hadron Form Factors: From Basic Phenomenology to QCD Sum Rules* (CRC Press, 2020).
- [50] C. W. Bauer, S. Fleming, D. Pirjol, I. Z. Rothstein, and I. W. Stewart, Phys. Rev. D **66**, 014017 (2002), arXiv:hep-ph/0202088.
- [51] I. Z. Rothstein, Phys. Rev. D **70**, 054024 (2004), arXiv:hep-ph/0301240.
- [52] H.-n. Li and G. F. Sterman, Nucl. Phys. B **381**, 129 (1992).

- [53] H.-n. Li, Y.-L. Shen, Y.-M. Wang, and H. Zou, Phys. Rev. D **83**, 054029 (2011), arXiv:1012.4098 [hep-ph].
- [54] H.-N. Li, Y.-L. Shen, and Y.-M. Wang, JHEP **02**, 008 (2013), arXiv:1210.2978 [hep-ph].
- [55] H.-N. Li, Y.-L. Shen, and Y.-M. Wang, JHEP **01**, 004 (2014), arXiv:1310.3672 [hep-ph].
- [56] H.-n. Li and Y.-M. Wang, JHEP **06**, 013 (2015), arXiv:1410.7274 [hep-ph].
- [57] Y. Aoki *et al.* (Flavour Lattice Averaging Group (FLAG)), Eur. Phys. J. C **82**, 869 (2022), arXiv:2111.09849 [hep-lat].
- [58] V. M. Braun and I. E. Filyanov, Z. Phys. C **44**, 157 (1989).
- [59] V. M. Braun and I. E. Filyanov, Z. Phys. C **48**, 239 (1990).
- [60] V. M. Braun, G. P. Korchemsky, and D. Müller, Prog. Part. Nucl. Phys. **51**, 311 (2003), arXiv:hep-ph/0306057.
- [61] T. Hahn, Comput. Phys. Commun. **140**, 418 (2001), arXiv:hep-ph/0012260.
- [62] G. Passarino and M. J. G. Veltman, Nucl. Phys. B **160**, 151 (1979).
- [63] F. Feng, Comput. Phys. Commun. **183**, 2158 (2012), arXiv:1204.2314 [hep-ph].
- [64] A. V. Smirnov, JHEP **10**, 107 (2008), arXiv:0807.3243 [hep-ph].
- [65] J. Gao, T. Huber, Y. Ji, and Y.-M. Wang, Phys. Rev. Lett. **128**, 062003 (2022), arXiv:2106.01390 [hep-ph].
- [66] J. Gao, T. Huber, Y. Ji, and Y.-M. Wang, SciPost Phys. Proc. **7**, 022 (2022), arXiv:2110.14776 [hep-ph].
- [67] A. V. Kotikov, Phys. Lett. B **254**, 158 (1991).
- [68] T. Gehrmann and E. Remiddi, Nucl. Phys. B **580**, 485 (2000), arXiv:hep-ph/9912329.
- [69] J. M. Henn, Phys. Rev. Lett. **110**, 251601 (2013), arXiv:1304.1806 [hep-th].
- [70] R. N. Lee, JHEP **04**, 108 (2015), arXiv:1411.0911 [hep-ph].
- [71] R. N. Lee, Comput. Phys. Commun. **267**, 108058 (2021), arXiv:2012.00279 [hep-ph].
- [72] X. Liu and Y.-Q. Ma, Comput. Phys. Commun. **283**, 108565 (2023), arXiv:2201.11669 [hep-ph].
- [73] X. Liu, Y.-Q. Ma, and C.-Y. Wang, Phys. Lett. B **779**, 353 (2018), arXiv:1711.09572 [hep-ph].
- [74] X. Liu and Y.-Q. Ma, Phys. Rev. D **105**, L051503 (2022), arXiv:2107.01864 [hep-ph].
- [75] H. Ferguson, D. Bailey, and S. Arno, Mathematics of Computation **68**, 351 (1999).
- [76] H. R. Ferguson, D. H. Bailey, and P. B. Borwein, *A polynomial time, numerically stable integer relation algorithm*, Tech. Rep. (1998).
- [77] A. B. Goncharov, Math. Res. Lett. **5**, 497 (1998), arXiv:1105.2076 [math.AG].
- [78] A. B. Goncharov, (2001), arXiv:math/0103059.
- [79] P. Breitenlohner and D. Maison, Commun. Math. Phys. **52**, 11 (1977).
- [80] G. Bonneau, Nucl. Phys. B **167**, 261 (1980).
- [81] G. Bonneau, Nucl. Phys. B **171**, 477 (1980).
- [82] J. C. Collins, *Renormalization*, Cambridge Monographs on Mathematical Physics, Vol. 26 (Cambridge University Press, Cambridge, 2023).
- [83] M. Beneke and S. Jager, Nucl. Phys. B **751**, 160 (2006), arXiv:hep-ph/0512351.
- [84] F. Herzog, B. Ruijl, T. Ueda, J. A. M. Vermaasen, and A. Vogt, JHEP **02**, 090 (2017), arXiv:1701.01404 [hep-ph].
- [85] T. Luthe, A. Maier, P. Marquard, and Y. Schröder, JHEP **10**, 166 (2017), arXiv:1709.07718 [hep-ph].
- [86] K. G. Chetyrkin, G. Falcioni, F. Herzog, and J. A. M. Vermaasen, JHEP **10**, 179 (2017), [Addendum: JHEP 12, 006 (2017)], arXiv:1709.08541 [hep-ph].
- [87] M. H. Sarmadi, Phys. Lett. B **143**, 471 (1984).
- [88] F. M. Dittes and A. V. Radyushkin, Phys. Lett. B **134**, 359 (1984).
- [89] G. R. Katz, Phys. Rev. D **31**, 652 (1985).
- [90] S. V. Mikhailov and A. V. Radyushkin, Nucl. Phys. B **254**, 89 (1985).
- [91] A. V. Belitsky, D. Mueller, and A. Freund, Phys. Lett. B **461**, 270 (1999), arXiv:hep-ph/9904477.
- [92] M. J. Dugan and B. Grinstein, Phys. Lett. B **256**, 239 (1991).
- [93] S. Herrlich and U. Nierste, Nucl. Phys. B **455**, 39 (1995), arXiv:hep-ph/9412375.
- [94] A. J. Buras and P. H. Weisz, Nucl. Phys. B **333**, 66 (1990).
- [95] M. Jamin and A. Pich, Nucl. Phys. B **425**, 15 (1994), arXiv:hep-ph/9402363.
- [96] A. J. Buras, Phys. Rept. **1025** (2023), 10.1016/j.physrep.2023.07.002, arXiv:1102.5650 [hep-ph].
- [97] M. Beneke and S. Jager, Nucl. Phys. B **768**, 51 (2007), arXiv:hep-ph/0610322.
- [98] T. Becher and R. J. Hill, JHEP **10**, 055 (2004), arXiv:hep-ph/0408344.
- [99] R. J. Hill, T. Becher, S. J. Lee, and M. Neubert, JHEP **07**, 081 (2004), arXiv:hep-ph/0404217.
- [100] M. Beneke and D. Yang, Nucl. Phys. B **736**, 34 (2006), arXiv:hep-ph/0508250.
- [101] G. Buchalla, A. J. Buras, and M. E. Lautenbacher, Rev. Mod. Phys. **68**, 1125 (1996), arXiv:hep-ph/9512380.
- [102] A. J. Buras, M. Misiak, and J. Urban, Nucl. Phys. B **586**, 397 (2000), arXiv:hep-ph/0005183.
- [103] Y.-M. Wang and Y.-L. Shen, Nucl. Phys. B **898**, 563 (2015), arXiv:1506.00667 [hep-ph].
- [104] Y.-M. Wang and Y.-L. Shen, JHEP **12**, 037 (2017), arXiv:1706.05680 [hep-ph].
- [105] J. Gao, C.-D. Lü, Y.-L. Shen, Y.-M. Wang, and Y.-B. Wei, Phys. Rev. D **101**, 074035 (2020), arXiv:1907.11092 [hep-ph].
- [106] Y.-K. Huang, B.-X. Shi, Y.-M. Wang, and X.-C. Zhao, (2024), arXiv:2407.18724 [hep-ph].
- [107] H.-D. Li, C.-D. Lü, C. Wang, Y.-M. Wang, and Y.-B. Wei, JHEP **04**, 023 (2020), arXiv:2002.03825 [hep-ph].
- [108] B.-Y. Cui, Y.-K. Huang, Y.-M. Wang, and X.-C. Zhao, Phys. Rev. D **108**, L071504 (2023), arXiv:2301.12391 [hep-ph].
- [109] C. Duhr and F. Dulat, JHEP **08**, 135 (2019), arXiv:1904.07279 [hep-th].
- [110] J. A. M. Vermaasen, Int. J. Mod. Phys. A **14**, 2037 (1999), arXiv:hep-ph/9806280.
- [111] V. A. Smirnov, *Analytic tools for Feynman integrals*, Vol. 250 (2012).
- [112] V. M. Braun, A. N. Manashov, S. Moch, and M. Strohmaier, JHEP **06**, 037 (2017), arXiv:1703.09532 [hep-ph].
- [113] M. Strohmaier, *Conformal symmetry breaking and evolution equations in Quantum Chromodynamics*, Ph.D. thesis, Regensburg U. (2018).
- [114] S. J. Brodsky and G. F. de Teramond, Phys. Rev. D **77**,

- 056007 (2008), arXiv:0707.3859 [hep-ph].
- [115] A. Khodjamirian, B. Melić, Y.-M. Wang, and Y.-B. Wei, JHEP **03**, 016 (2021), arXiv:2011.11275 [hep-ph].
- [116] G. S. Bali, V. M. Braun, S. Bürger, M. Göckeler, M. Gruber, F. Hutzler, P. Korcyl, A. Schäfer, A. Sternbeck, and P. Wein (RQCD), JHEP **08**, 065 (2019), [Addendum: JHEP 11, 037 (2020)], arXiv:1903.08038 [hep-lat].
- [117] S. Cheng, A. Khodjamirian, and A. V. Rusov, Phys. Rev. D **102**, 074022 (2020), arXiv:2007.05550 [hep-ph].
- [118] V. M. Braun, A. Khodjamirian, and M. Maul, Phys. Rev. D **61**, 073004 (2000), arXiv:hep-ph/9907495.
- [119] J. Bijnens and A. Khodjamirian, Eur. Phys. J. C **26**, 67 (2002), arXiv:hep-ph/0206252.
- [120] A. Khodjamirian, T. Mannel, N. Offen, and Y. M. Wang, Phys. Rev. D **83**, 094031 (2011), arXiv:1103.2655 [hep-ph].
- [121] A. P. Bakulev, S. V. Mikhailov, and N. G. Stefanis, Phys. Lett. B **508**, 279 (2001), [Erratum: Phys.Lett.B 590, 309–310 (2004)], arXiv:hep-ph/0103119.
- [122] S. V. Mikhailov, A. V. Pimikov, and N. G. Stefanis, Phys. Rev. D **93**, 114018 (2016), arXiv:1604.06391 [hep-ph].
- [123] N. G. Stefanis, Phys. Rev. D **102**, 034022 (2020), arXiv:2006.10576 [hep-ph].
- [124] S. V. Mikhailov and A. V. Radyushkin, Phys. Rev. D **45**, 1754 (1992).
- [125] I. Cloet, X. Gao, S. Mukherjee, S. Syritsyn, N. Karthik, P. Petreczky, R. Zhang, and Y. Zhao, (2024), arXiv:2407.00206 [hep-lat].
- [126] X. Ji, Phys. Rev. Lett. **110**, 262002 (2013), arXiv:1305.1539 [hep-ph].
- [127] X. Ji, Sci. China Phys. Mech. Astron. **57**, 1407 (2014), arXiv:1404.6680 [hep-ph].
- [128] X. Ji, Y.-S. Liu, Y. Liu, J.-H. Zhang, and Y. Zhao, Rev. Mod. Phys. **93**, 035005 (2021), arXiv:2004.03543 [hep-ph].
- [129] S. S. Agaev, V. M. Braun, N. Offen, and F. A. Porkert, Phys. Rev. D **83**, 054020 (2011), arXiv:1012.4671 [hep-ph].
- [130] B. Melic, B. Nizic, and K. Passek, Phys. Rev. D **65**, 053020 (2002), arXiv:hep-ph/0107295.
- [131] N. G. Stefanis, Eur. Phys. J. direct **1**, 7 (1999), arXiv:hep-ph/9911375.
- [132] M. Mojaza, S. J. Brodsky, and X.-G. Wu, Phys. Rev. Lett. **110**, 192001 (2013), arXiv:1212.0049 [hep-ph].
- [133] X.-G. He, T. Li, X.-Q. Li, and Y.-M. Wang, Phys. Rev. D **74**, 034026 (2006), arXiv:hep-ph/0606025.
- [134] C.-D. Lu, Y.-M. Wang, H. Zou, A. Ali, and G. Kramer, Phys. Rev. D **80**, 034011 (2009), arXiv:0906.1479 [hep-ph].
- [135] Y.-M. Wang and Y.-L. Shen, JHEP **02**, 179 (2016), arXiv:1511.09036 [hep-ph].
- [136] L. Di Giustino, S. J. Brodsky, P. G. Ratcliffe, X.-G. Wu, and S.-Q. Wang, Prog. Part. Nucl. Phys. **135**, 104092 (2024), arXiv:2307.03951 [hep-ph].
- [137] H.-T. Ding, X. Gao, A. D. Hanlon, S. Mukherjee, P. Petreczky, Q. Shi, S. Syritsyn, R. Zhang, and Y. Zhao, Phys. Rev. Lett. **133**, 181902 (2024), arXiv:2404.04412 [hep-lat].
- [138] V. M. Braun and A. Khodjamirian, Phys. Lett. B **718**, 1014 (2013), arXiv:1210.4453 [hep-ph].
- [139] Y.-M. Wang, JHEP **09**, 159 (2016), arXiv:1606.03080 [hep-ph].
- [140] Y.-M. Wang and Y.-L. Shen, JHEP **05**, 184 (2018), arXiv:1803.06667 [hep-ph].
- [141] M. Beneke, V. M. Braun, Y. Ji, and Y.-B. Wei, JHEP **07**, 154 (2018), arXiv:1804.04962 [hep-ph].
- [142] A. Khodjamirian, B. Melić, and Y.-M. Wang, Eur. Phys. J. ST **233**, 271 (2024), arXiv:2311.08700 [hep-ph].
- [143] V. M. Braun, A. N. Manashov, S. Moch, and J. Schoenleber, Phys. Rev. D **104**, 094007 (2021), arXiv:2106.01437 [hep-ph].
- [144] V. M. Braun, A. Lenz, N. Mahnke, and E. Stein, Phys. Rev. D **65**, 074011 (2002), arXiv:hep-ph/0112085.
- [145] V. M. Braun, A. Lenz, and M. Wittmann, Phys. Rev. D **73**, 094019 (2006), arXiv:hep-ph/0604050.
- [146] I. V. Anikin, V. M. Braun, and N. Offen, Phys. Rev. D **88**, 114021 (2013), arXiv:1310.1375 [hep-ph].
- [147] P. Böer, *QCD Factorisation in Exclusive Semileptonic B Decays: New Applications and Resummation of Rapidity Logarithms*, Ph.D. thesis, Siegen U. (2018).
- [148] G. Bell and T. Feldmann, Nucl. Phys. B Proc. Suppl. **164**, 189 (2007), arXiv:hep-ph/0509347.
- [149] G. Bell, *Higher order QCD corrections in exclusive charmless B decays*, Ph.D. thesis, Munich U. (2006), arXiv:0705.3133 [hep-ph].
- [150] P. Böer, G. Bell, T. Feldmann, D. Horstmann, and V. Shtabovenko, PoS **RADCOR2023**, 086 (2024), arXiv:2309.08410 [hep-ph].
- [151] D. Mueller, Phys. Rev. D **49**, 2525 (1994).
- [152] A. V. Belitsky and A. V. Radyushkin, Phys. Rept. **418**, 1 (2005), arXiv:hep-ph/0504030.
- [153] L.-B. Chen, W. Chen, F. Feng, and Y. Jia, Phys. Rev. Lett. **132**, 201901 (2024), arXiv:2312.17228 [hep-ph].
- [154] J. Aebischer, A. J. Buras, and J. Kumar, Phys. Rev. D **107**, 075007 (2023), arXiv:2202.01225 [hep-ph].
- [155] M. I. Buchoff and M. Wagman, Phys. Rev. D **93**, 016005 (2016), [Erratum: Phys.Rev.D 98, 079901 (2018)], arXiv:1506.00647 [hep-ph].
- [156] A. Buras, *Gauge Theory of Weak Decays* (Cambridge University Press, 2020).